

LAND USE AND LAND COVER (LULC) CLASSIFICATION WITH MACHINE LEARNING APPROACH USING ORTHOPHOTO DATA

(Klasifikasi Penggunaan Lahan dan Penutup Lahan dengan Pendekatan Machine Learning Menggunakan Data Orthophoto)

Mochamad Irwan Hariyono¹, Rokhmatuloh², Ratna Sari Dewi³

¹Research Center for Geospatial, National Research and Innovation Agency (BRIN)

²Department of Geography, Faculty of Mathematics and Natural Sciences, University of Indonesia

³Geospatial Information Agency

Jl. Raya Jakarta- Bogor Km 46. Cibinong, Bogor Regency, West Java, 16911

E-mail: moch053@brin.go.id

Diterima: 4 Februari 2023; Direvisi: 26 Maret 2023; Disetujui untuk Dipublikasikan: 29 April 2023

ABSTRACT

The use of remote sensing technology is growing, one application of which is the analysis of changes in land use and land cover (LULC). LULC information is needed for various analyses related to the Earth's surface. Various types of data are used in the analysis of the Earth's surface by utilizing remote sensing data. The purpose of this study is to classify LULC using a machine learning approach with orthophoto data. The research location is Tanjung Karang Village, Mataram, West Nusa Tenggara. The method used for the classification process is a machine learning algorithm called Support Vector Machine (SVM). A band slicing process is carried out to separate the bands in the orthophoto data, namely the Red, Green, Blue, and Near Infra Red (NIR) bands. The Normalized Difference Water Index (NDWI) band is used for the analysis of water bodies, which is a reflection of the Red and NIR bands. The classification scheme applied in this research is to compare the classification between single band and band combination to find the best classification result. The results of this study indicate that classification with a combination of bands has better accuracy. Classification with a single band has an average accuracy of below 55%, while a combination of bands has an average accuracy of above 60%. The classification result with the highest accuracy value is the R-B-NDWI band combination with a value of 71.81%.

Keywords: LULC, machine learning, orthophoto, remote sensing

ABSTRAK

Penggunaan teknologi penginderaan jauh semakin berkembang, salah satu aplikasinya adalah analisis perubahan penggunaan dan tutupan lahan (LULC). Informasi LULC dibutuhkan untuk berbagai analisis terkait permukaan bumi. Berbagai jenis data digunakan dalam analisis permukaan bumi dengan memanfaatkan data penginderaan jauh. Tujuan dari penelitian ini adalah untuk mengklasifikasikan LULC dengan pendekatan machine learning menggunakan data orthophoto. Lokasi penelitian adalah Desa Tanjung Karang, Mataram, Nusa Tenggara Barat. Metode yang digunakan untuk proses klasifikasi adalah algoritma machine learning yaitu Support Vector Machine (SVM). Dilakukan proses pemisahan band (band slicing) pada data orthophoto yaitu Red, Green, Blue, dan Near Infra Red (NIR). Band Normalized Difference Water Index (NDWI) digunakan untuk analisis badan air yang merupakan refleksi dari band Red dan NIR. Skema klasifikasi yang diterapkan dalam penelitian ini adalah membandingkan klasifikasi antara satu band dan kombinasi band untuk mendapatkan hasil klasifikasi terbaik. Hasil penelitian ini menunjukkan bahwa klasifikasi dengan kombinasi band memiliki akurasi yang lebih baik. Klasifikasi dengan satu band memiliki akurasi rata-rata di bawah 55%, sedangkan kombinasi band memiliki akurasi rata-rata di atas 60%. Hasil klasifikasi dengan nilai akurasi tertinggi adalah kombinasi band R-B-NDWI dengan nilai 71,81%.

Kata kunci: LULC, machine learning, orthophoto, penginderaan jauh

INTRODUCTION

Technological developments, such as remote sensing, have become increasingly significant. Remote sensing technology can provide information on land cover, which includes physical materials on the earth's surface, such as water, vegetation, impermeable surfaces, and bare soil (Cai et al., 2018). Currently, the most common data sources for land cover analysis are satellite imagery and aerial photography. Aerial

photography is particularly useful for accurately analyzing changes in land cover (Huang et al., 2019). Remote sensing data collected from satellite and aerial sensors with very high spatial resolution is now widely available, with data resolution available down to sub-meter precision.

Land use/land cover (LULC) information is crucial for various purposes, such as thematic requirements, infrastructure planning, disaster management, and spatial planning. To obtain this information, available data sources are processed.

Remote sensing data, including satellite imagery, aerial photographs, and lidar, is commonly used for the extraction of land use and land cover classes. The use of this data is often cheaper than using terrestrial survey methods to obtain information on a large scale with wide area coverage.

One of the key tasks in utilizing remote sensing data is extracting information, which typically involves land use/land cover (LULC) classification. The extraction process can be performed manually through on-screen digitization, but this can be costly and time-consuming. To overcome these challenges, software applications and machine learning and deep learning algorithms have been developed for remote sensing data processing. Machine learning algorithms are particularly effective because they can be adapted to specific data processing needs, unlike rule-based software.

Classification is interesting research themes since the last two decades, especially in remote sensing hyperspectral data. Many development algorithms for LULC classification use orthophoto data (Ramanath et al., 2019; Jamil & Bayram, 2018; López-jiménez et al., 2019). The extraction technique in machine learning is generally supervised classification by training a model to be used for other input data. Classification of LULC using raster data generally uses object-based and pixel-based methods.

Aerial photography is a part of remote sensing technology with high resolution. The result of processing aerial photos (raw data) is Orthophoto, which is an aerial photo that has undergone a rectification process, or a photo image whose appearance has been enforced, meaning that the coordinates have been adjusted to the existing field.

Interpretation of aerial photographs generally still uses visual interpretation manually by digitizing on screen. Besides that, field surveys are also carried out to validate the results of the interpretation. This is quite time-consuming and expensive (Thasveen & Suresh, 2021). Because of that, there is a need for innovation to overcome this, one of which is by conducting various studies related to accelerating mapping by developing machine learning algorithms to achieve automation or semi-automation of mapping.

Several previous studies have used orthophoto data for LULC extraction and classification, including tree species classification and extraction (Jamil & Bayram, 2018), land cover classification using machine learning (Jozdani et al. 2019), object recognition with deep learning and land cover reconstruction (Ratajczak et al., 2019).

The purpose of this research is to classify land use/cover using orthophoto data with machine learning algorithms. The machine learning method utilized in this research is the Support Vector Machine (SVM), which was chosen due to its development in multi-class classification. Previous

research results (Ahmad et al., 2018) have shown that the SVM algorithm produces higher classification accuracy compared to other algorithms such as Neural Network and Classification and Regression Trees. Additionally, (Noi & Kappas, 2017) found SVM to have advantages over Random Forest and K-Nearest Neighbor algorithms and to be suitable for multispectral data classification such as Sentinel-2 Multispectral Instrument (MSI).

In the machine learning community, SVM is one of the most commonly used classifiers to categorize data using an optimal separator hyperplane (Cortes & Vapnik, 1995). One of the main advantages of using SVM for remote sensing data applications is its ability to handle high-dimensional data using relatively few training samples. Beside that, the importance of using SVM in data classification lies in its ability to overcome the problems of "overfitting" and "noise" in the data. Overfitting occurs when the model is too complex and capable of capturing the uniqueness of the training dataset, but cannot be applied effectively to new data. SVM can help overcome overfitting by optimizing the margin (closest distance between the decision boundary and data points from different classes) which can help clearly distinguish between different classes.

METHOD

The LULC classification in this study uses aerial photos as the primary data. The data used in the study consists of orthophotos of the Tanjung Karang Village area in Mataram City, Lombok. The aerial photo data was acquired by the Geospatial Information Agency (BIG) in 2016. Data acquisition is carried out using specially designed aircraft for aerial photography, which is able to perform work according to predetermined specifications.

The aerial camera used is a digital metric aerial camera designed for aerial surveying with a Normal Angle lens type, equipped with Kinematic Global Positioning System (GPS) and Inertial Measurement Unit (IMU) and has radiometric spectrum capabilities that can cover Red, Green, Blue (RGB) and Near InfraRed (NIR). The data has a resolution of 0.15 m and was acquired using a LEICA RCD 30 camera (60 mpix), a medium format camera with a GSD of 11.09 cm.

The location was selected based on the diverse LULC objects in the area, with the aim of ensuring that the results of the classification using the machine learning approach would be sufficiently representative of other areas with similar LULC conditions. The research area covers approximately 2.57 km². The orthophoto data for the research locations is shown in **Figure 1**. In this study, the classification process employs machine learning based on Support Vector Machine (SVM) technology, and utilizing spectral information from the orthophoto data. It is primarily used for binary classification, as shown in **Figure 2**.

Figure 2 has meaning, where green dots denote the samples of class A, blue dots denote the samples of class B, red circles denote the support vector and purple dots denote the noise samples in (b). This algorithm utilizes non-parametric methods and does not make assumptions about the distribution of data. The objective of SVM is to find the hyperplane with the maximum margin, which is the distance between the hyperplane and the closest points from each class. This approach aims to find the optimal hyperplane that can correctly classify new data points with high accuracy. The main goal is to achieve the highest possible classification performance with a low error rate and the best generalization ability for new data, as shown in **Equation (1)**.

$$f(x) = [\omega \cdot \varphi(x) + b] \dots\dots\dots(1)$$

where:

- $f(x)$ = SVM function
- ω = orientation hyperplane

- $\varphi(x)$ = non-linear mapping function
- b = hyperplane distance

The Kernel function (**Equation (2)**) was used in SVM to assume that the separation of nonlinear data is linear in a high-dimensional space (Jamil & Bayram, 2018).

$$K(x_i, x_j) = \exp\left(-\frac{1}{\sigma^2} \|x_i - x_j\|\right) \dots\dots\dots(2)$$

where:

- $K(x_i, x_j)$ = Kernel function
- σ = parameter value

Qin, (2015) states that SVM has the advantage of being able to handle high-dimensional data with a small number of training samples, and can produce accurate classification results. However, under these conditions, when the number of occur features is greater than the number of experimental data (training sample), classification failure may.

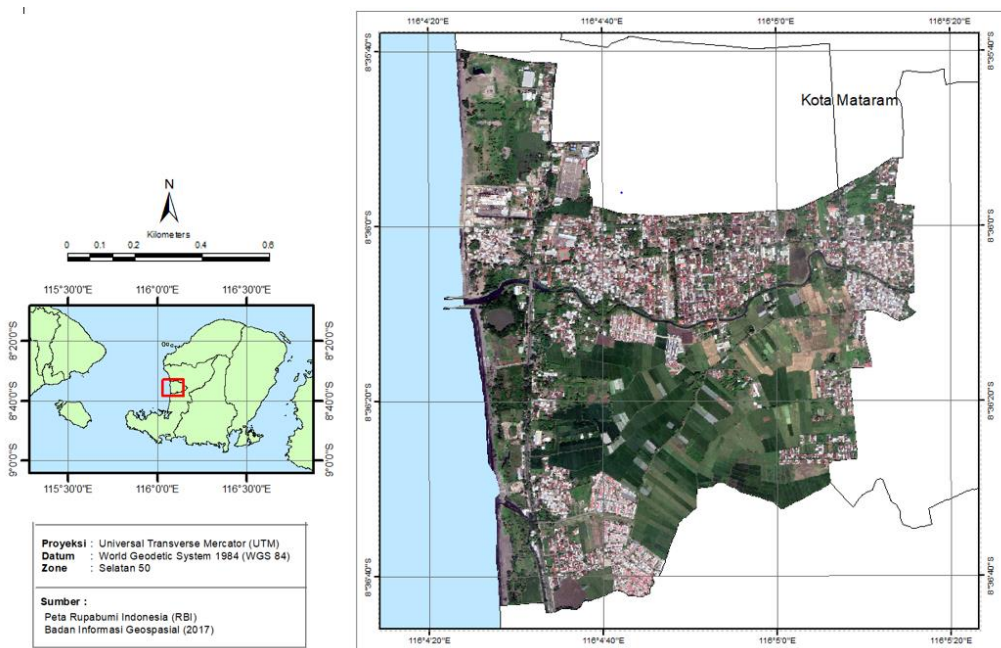
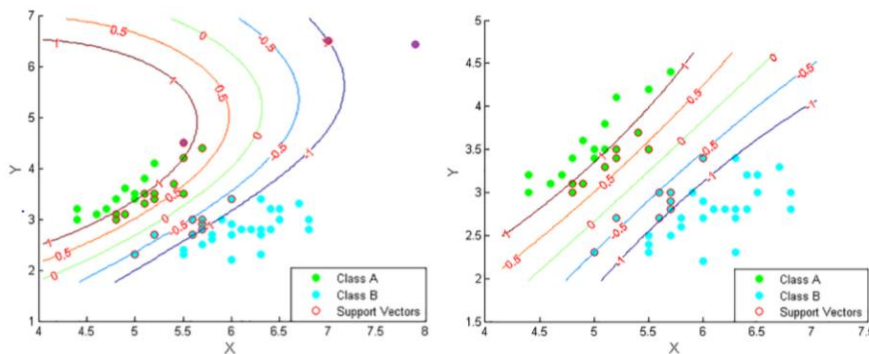


Figure 1. Study area, Tanjung Karang Village, Mataram City, Lombok.



Source : Liu & Huang, (2019)

Figure 2. Visualization of SVM classification.

To overcome these problems, the Kernel Radial Basis Function (RBF) function is generally used to efficiently train data and improve accuracy results Dumitru et al., (2016). The process of tuning the two free parameters of this classifier, which are C (the penalty parameter of the error term) and ξ (the margin of tolerance), usually involves cross-validation of the training data and grid-search to select the optimal values. The ξ algorithm as in **Equation (3)**.

$$yi(\omega, \varphi(xi) + b) + \xi i \geq 1 \dots\dots\dots(3)$$

$$\xi i \geq 0, \quad 1 \leq i \leq n$$

where:

- y_i = dataset training
- ω = hyperplane orientation
- $\varphi(x_i)$ = non-linear mapping function
- b = hyperplane distance
- ξ = positive slack variable
- n = number of samples

In addition, SVM is more efficient for classification. However, normalization of differences in dataset features (scale normalization) greatly affects the classification results (Pal et al., 2020). The analysis of processing results is carried out based on several variables, namely the level of accuracy, precision, and similarity to the reference data. The land cover classification is based on reference data, which consists of buildings, vegetation (high and low), bare land, roads, and water.

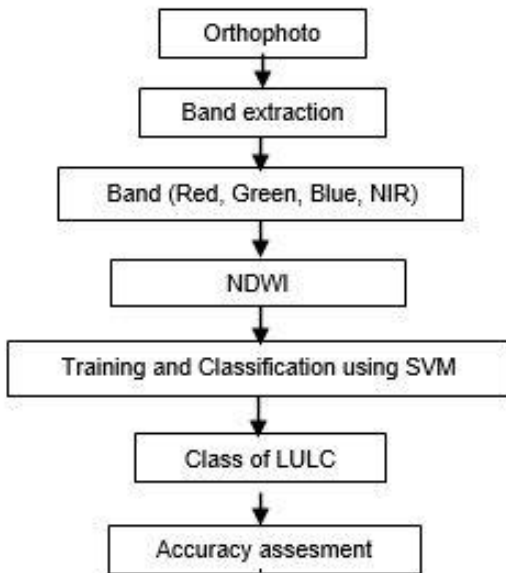


Figure 3. Research workflow.

The orthophoto data used in this study has four bands, namely red, green, blue (RGB), and Near-Infra Red (NIR), with a resolution of 0.15 m. The process of separating the bands (band slicing) is carried out using an algorithm in Python. Orthophoto data processing can be seen in **Figure 3**. The band extraction process aims to extract spectral, spatial, textural, and vegetation index information. The bands used for the classification

process consist of R, G, B, and NIR. For the analysis of water bodies using the NDWI band, this band uses reflections from G and NIR band radiation.

NDWI is used to sharpen water body objects and eliminate the appearance of land and vegetation objects (Mcfeeters, 1996). Another study (Chai et al., 2020) used NDWI for river and lake extraction on Landsat imagery. The NDWI equation is shown in **Equation (4)**.

With data characteristics that have high spatial resolution, an increase in classification accuracy is expected. The classification scheme applied was classification with a single band (R, G, B, NDWI) and a combination of bands (**Table 1**). In this study, a combination of 3 bands was used, referring to previous studies (El-ashmawy et al., 2011). Generally, this combination is used in LULC classification because it can provide enough information to distinguish between natural features such as vegetation, water, and land surface. The use of a 3-band combination also allows for the generation of a color image that can aid in visualizing and understanding the classification results. Additionally, using only 3 bands can reduce data complexity and speed up the classification process, especially for large areas that require fast processing times.

$$NDWI = \frac{Green - NIR}{Green + NIR} \dots\dots\dots(4)$$

Table 1. Band combination for LULC classification using orthophoto data.

Band Combination		
R	G	B
R	G	NIR
R	G	NDWI
R	B	NIR
R	B	NDWI
R	NIR	NDWI
G	B	NIR
G	B	NDWI
G	NIR	NDWI
B	NIR	NDWI

SVM has advantages compared to other machine learning methods, such as the use of limited training data and producing good output using spectral data (Xu et al., 2018). The data training process in this study was carried out by taking samples from each land cover class. This sample data is used as a reference in classifying pixel values that represent the appearance of LULC from the data source. Training data collection was carried out in an evenly distributed manner for each LULC class, with approximately

25 samples for each class, namely class of vegetation, buildings, roads, bare land, water bodies. Data sampling was based on similarities (color, hue, association, and texture) for the class or same object. For the training data and accuracy test data in this study, they were carried out in the same location area.

The accuracy test of the classification results used the Indonesia Topographic Map (RBI) scale 1:5000 in 2017 as the reference data. To assess the accuracy of the classification results, the Kappa Coefficient and Overall Accuracy were calculated based on the Confusion Matrix. This classification test was carried out to evaluate the performance of the Support Vector Machine algorithm using the reference data.

The classification results were compared with the 1:5000 scale RBI map to obtain the overall accuracy value based on the principles of the confusion matrix. The confusion matrix was used to evaluate the classification results for different LULC conditions (Foody, 2002), and an illustration of the confusion matrix can be seen in **Figure 4**. The equation of OA, producer accuracy and user accuracy are shown in **Equation 5**, **Equation 6**, and **Equation 7**.

k,k	A	B	C	...	q	Σ
A	n _{AA}	n _{AB}	n _{AC}	...	n _{Aq}	n _{A+}
B	n _{BA}	n _{BB}	n _{BC}	...	n _{Bq}	n _{B+}
C	n _{CA}	n _{CB}	n _{CC}	...	n _{Cq}	n _{C+}
⋮	⋮	⋮	⋮	...	⋮	⋮
q	n _{qA}	n _{qB}	n _{qC}	...	n _{qq}	n _{q+}
Σ	n _{+A}	n _{+B}	n _{+C}	...	n _{+q}	n

Source: Foody (2002), Reprocessed.
Figure 4. Confusion matrix to calculate overall accuracy (OA).

$$\text{Overall Accuracy} = \frac{\sum_{k=1}^q a_{kk}}{n} \times 100 \dots \dots \dots (5)$$

$$\text{User Accuracy} = \frac{n_{kk}}{n_{k+}} \times 100 \dots \dots \dots (6)$$

$$\text{Producer Accuracy} = \frac{n_{kk}}{n_{+k}} \times 100 \dots \dots \dots (7)$$

There is another aspect to accuracy testing, which does not involve using specific standards or parameters, but by documenting the time required at each stage of the process being carried out and comparing it with empirical data processing experience.

RESULTS AND DISCUSSION

The extraction results from the orthophoto data include the R, G, B, and NIR bands, which can be separated for further geospatial analysis. These bands are used to carry out the classification process using single band and combination band schemes with the SVM method

approach. In this scheme, the aim is to determine how well the results obtained from the LULC classification process using a single band compare to the utilization of band combinations. This is because each band has its own advantages and limitations for LULC analysis. In this study, a minimum of 25 samples were utilized for each LULC class during the machine learning process. The total for all LULC sampling is approximately 150 samples. The extraction results for the single band scheme can be seen in **Figure 5**.

A new band was derived from the extraction results for water body analysis in image data, called NDWI, which is derived from the G and NIR reflection bands. The NDWI bands can be seen in **Figure 6**. In previous studies using satellite imagery of water bodies (Chen et al., 2009), NDWI results are shown in bright colors or look brighter. However, in this study, the appearance and index values for river objects (bodies of water), asphalt roads, and shadows are almost the same because they appear black in natural colors.

The first classification process used the single band scheme, including the R, G, B, and NDWI bands. The classification results for each band can be seen in **Figure 7** (a, b, c, d). The classification results indicate that the use of a single band is insufficient to accurately identify all LULC classes. As a result, some classes may be misclassified as other classes.

Table 2. Overall accuracy value of single band classification.

Band	Overall Accuracy (OA)
R	55.86 %
G	49.50 %
B	50.08 %
NDWI	49.58 %

In the Red band, the classification results were close to the specified classes, as buildings, vegetation, roads, and bare land were identified. However, for the other bands, the classification results mostly only identified building and vegetation classes. The overall accuracy calculation results for the single band classification can be seen in **Table 2**.

Table 3. Overall accuracy value of band combination.

Band Combination			Overall Accuracy (OA)
R	G	B	71.73 %
R	G	NIR	61.32 %
R	G	NDWI	61.65 %
R	B	NIR	63.55 %
R	B	NDWI	71.81 %
R	NIR	NDWI	61.40 %
G	B	NIR	63.71 %

Band Combination			Overall Accuracy (OA)
G	B	NDWI	62.80 %
G	NIR	NDWI	50.00 %
B	NIR	NDWI	63.05 %

The next step is the classification process that employs a band combination scheme. The RGB and NDWI band combination was chosen because it can distinguish several classes that cannot be distinguished by a single band, such as water bodies, vegetation, and urban areas. This process revealed that classification using band combinations yielded better average accuracy

values than the single-band scheme. **Table 3** shows the overall accuracy value of the band combination. For the results of the confusion matrix of the highest OA values, we can see in **Table 4**.

Discussion or analysis of the classification results using a combination of bands only for the lowest and highest results. **Table 3** shows that the band combination with the lowest overall accuracy (OA) value is the G-NIR-NDWI combination, which yielded an accuracy of 50.00%. On the other hand, the R-B-NDWI band combination had the highest OA value with an accuracy of 71.81%, can be observed in **Figure 8**.

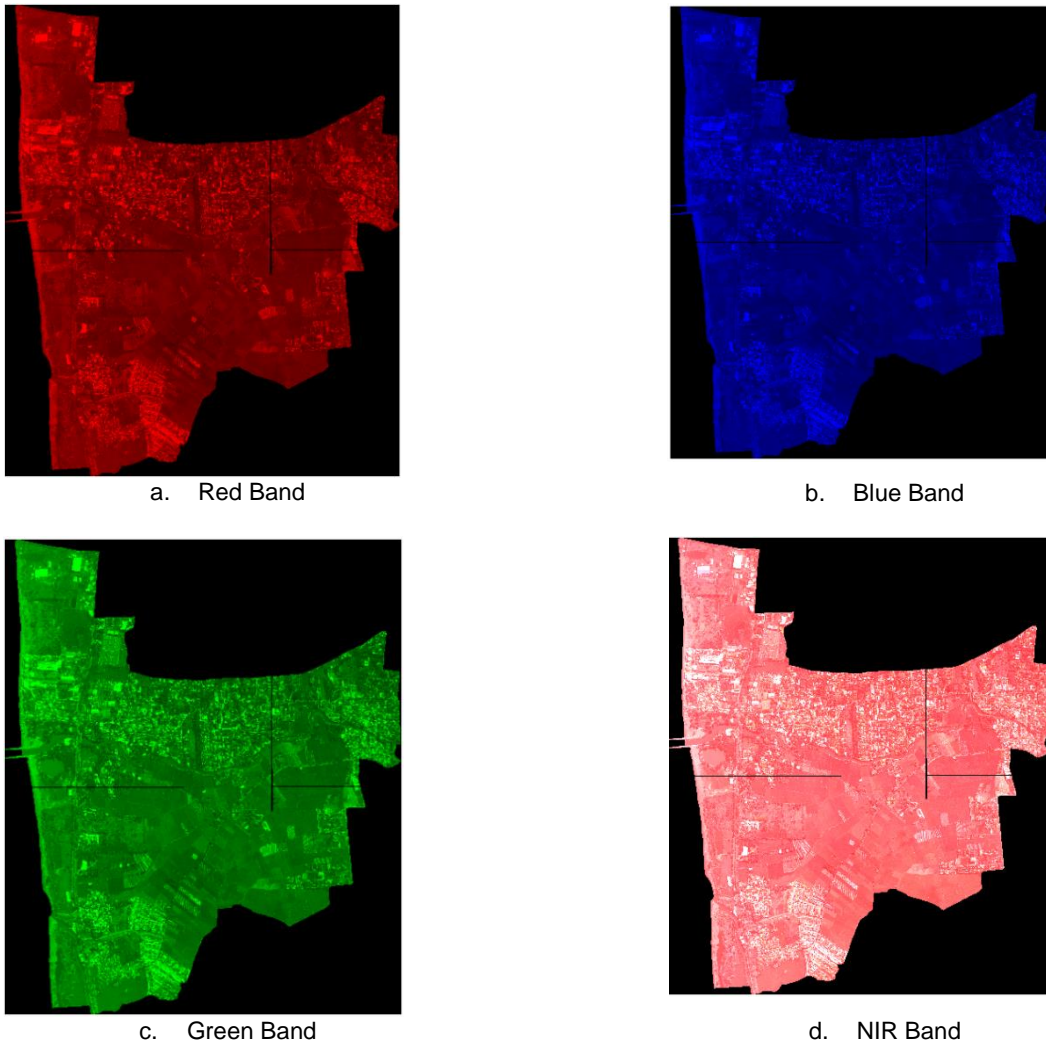


Figure 5. Result of single band ekstraktion.



Figure 6. NDWI Band.



Figure 7. LULC classification result using single band data.

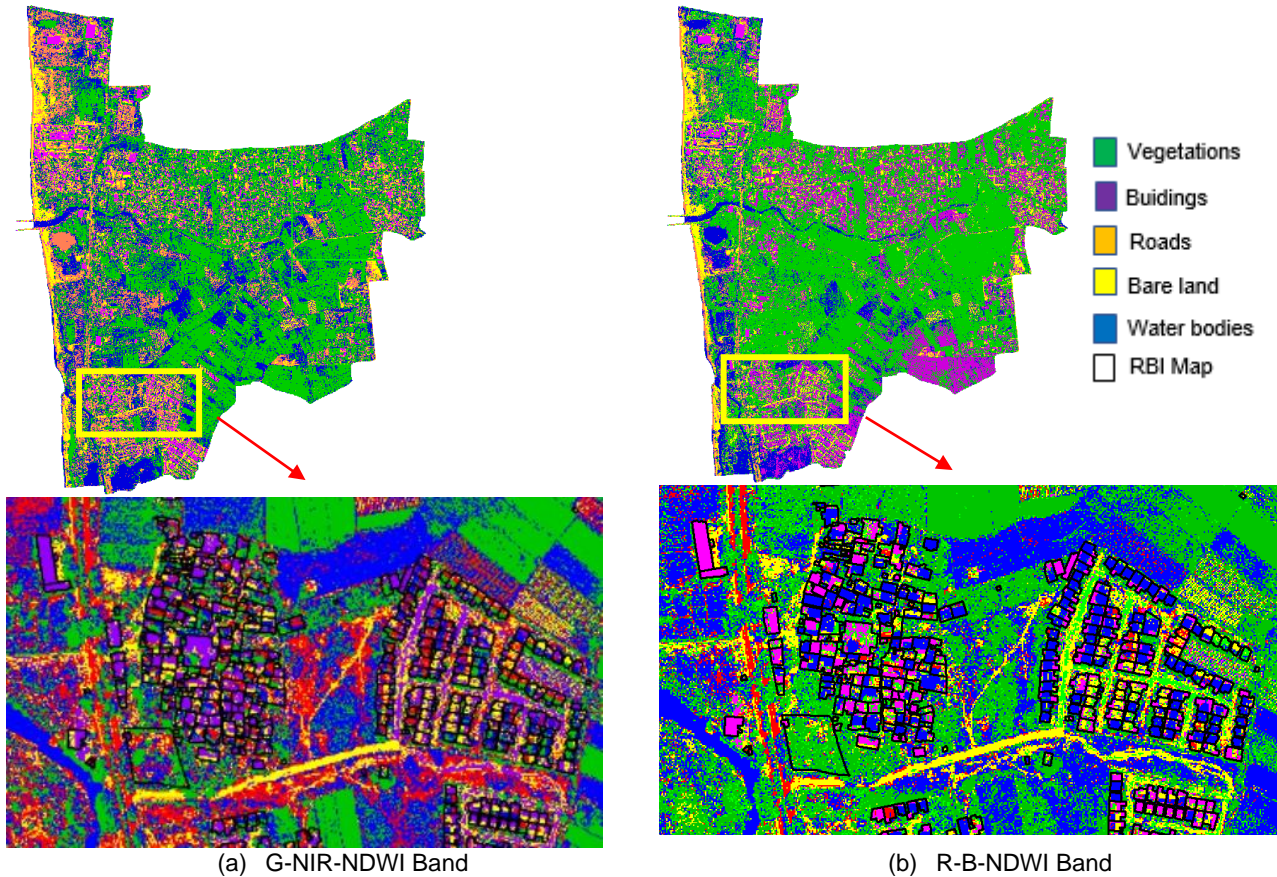


Figure 8. LULC classification result using combination band data.

Table 4. Confusion matrix for LULC classification using R-B-NDWI.

		Reference class					Total	User acc	Commission
		Vegetation	Buildings	Bare land	Roads	Water bodies			
Classification results	Vegetation	58	7	5	5	4	79	0.734	0.266
	Buildings	6	56	4	4	4	74	0.757	0.243
	Bare land	5	5	50	3	6	69	0.725	0.275
	Roads	4	2	4	42	2	54	0.778	0.222
	Water bodies	4	7	7	6	34	58	0.586	0.414
	Total	77	77	70	60	50	334		
Producer acc		0.753	0.727	0.714	0.700	0.680		Overall Accuracy	71.81%
Omission		0.247	0.273	0.286	0.300	0.320			

Figure 8 (a) G-NIR-NDWI band indicates that this combination is not representative for vegetation classes as most locations that should be classified as vegetation are identified as buildings. In the image section, we can analyze that the overlay result with the RBI map shows that the building class has been identified according to its location. Most of the vegetation classes are identified as water objects. The road object has not yet been classified. Bare land class has been identified, but it is still not well identified, some are still classified in other classes.

In the next image, Figure 8 (b) R-B-NDWI band shows better results, as all classes have been identified. In the image section, we can see that the overlay with the RBI map shows that the building class is already consistent with its area. The vegetation class has been identified well, although it is still identified as another class. The road and open land classes have also been identified, although some of them are still identified as another class. The results show that the classes of buildings, vegetation, roads, water bodies, and bare land have been identified more accurately compared to the single band classification.

CONCLUSION

The use of single band data in orthophoto classification resulted in poor LULC classification, with an OA value below 55%. In contrast, the band combination classification scheme yielded an average OA value above 60%. The best classification result was achieved using the R-B-NDWI band combination with an OA value is 71.81%, which identified most LULC classes accurately, although not all were identified perfectly. Nevertheless, this result suggests that the LULC classification process can be accelerated using SVM machine learning with a band combination scheme for orthophoto data.

ACKNOWLEDGEMENTS

We would like to express our gratitude to all parties who supported this research, particularly the Geospatial Information Agency (BIG) for facilitating the provision of data, as well as the reviewers and editors of the journal for their help in improving our manuscript.

REFERENCES

Ahmad, A., Hashim, U.K.M., Mohd, O., Abdullah, M.M., Sakidin, H. & Sufahani, S.F. (2018). Comparative analysis of support vector machine maximum likelihood and neural network classification on multispectral remote sensing data. *International Journal of Advanced Computer Science and Applications*, 9(9): 529-37. DOI: <https://doi.org/10.14569/IJACSA.2018.090966>.

Cai, L., Shi, W., Miao, Z. & Hao, M. (2018). Accuracy assessment measures for object extraction from remote sensing images. *Remote Sensing*, 10(2), 303, 1-13. DOI: <https://doi.org/10.3390/rs10020303>.

Chai, L., Jiang, H., Crow, W. T., Liu, S., Zhao, S., Liu, J. & Yang, S. (2020). Estimating corn canopy water content from normalized difference water index (NDWI): An optimized NDWI-Based scheme and its feasibility for retrieving corn VWC. *IEEE Transactions on Geoscience and Remote Sensing*, 59(10), 8168-8181. DOI: <https://doi.org/10.1109/TGRS.2020.3041039>.

Chen, Y., Su, W., Li, J. & Sun, Z. (2009). Hierarchical object oriented classification using very high resolution imagery and LIDAR data over urban areas. *Advances in Space Research*, 43(7), 1101-1110. DOI: <https://doi.org/10.1016/j.asr.2008.11.008>.

Cortes, C. & Vapnik, V. (1995). Support-Vector Networks. *Machine Learning* 20, 273-297. DOI: <https://doi.org/10.1007/BF00994018>.

Dumitru, C.O., Schwarz, G. & Datcu, M. (2016). Land cover semantic annotation derived from high-resolution SAR images. *IEEE Journal of Selected Topics in Applied Earth Observations and Remote Sensing*, 9(6), 2215-2232. DOI: <https://doi.org/10.1109/JSTARS.2016.2549557>.

El-ashmawy, N., Shaker, A. & Yan, W. (2011). Pixel vs object-based image classification techniques for LiDAR intensity data. *The International Archives of the Photogrammetry, Remote Sensing and Spatial Information Sciences*, XXXVIII-5(W12), 43-48. DOI: <https://doi.org/10.5194/isprsarchives-XXXVIII-5-W12-43-2011>.

https://doi.org/10.5194/isprsarchives-XXXVIII-5-W12-43-2011, 2011.

Foody, G.M. (2002). Status of land cover classification accuracy assessment. *Remote Sensing of Environment*, 80(1), 185-201. DOI: [https://doi.org/10.1016/S0034-4257\(01\)00295-4](https://doi.org/10.1016/S0034-4257(01)00295-4).

Huang, J., Zhang, X., Xin, Q., Sun, Y. & Zhang, P. (2019). Automatic building extraction from high-resolution aerial images and LiDAR data using gated residual refinement network. *ISPRS Journal of Photogrammetry and Remote Sensing*, 151(2019), 91-105. DOI: <https://doi.org/10.1016/j.isprsjprs.2019.02.019>.

Jamil, A. & Bayram, B. (2017). Tree species extraction and land use/cover classification from high-resolution digital orthophoto maps. *IEEE Journal of Selected Topics in Applied Earth Observations and Remote Sensing*, 11(1), 89-94. DOI: <https://doi.org/10.1109/JSTARS.2017.2756864>.

Jozdani, S.E., Johnson, B.A. & Chen, D. (2019). Comparing deep neural networks, ensemble classifiers, and support vector machine algorithms for object-based urban land use/land cover classification. *Remote Sensing*, 11(14), 1713, 1-24. DOI: <https://doi.org/10.3390/rs11141713>.

Liu, Y. & Huang, L. (2019). A novel ensemble support vector machine model for land cover classification. *International Journal of Distributed Sensor Networks*, 15(4), 1-9. DOI: <https://doi.org/10.1177/1550147719842732>.

López-Jiménez, E., Vasquez-Gomez, J.I., Sanchez-Acevedo, M.A., Herrera-Lozada, J.C. & Uriarte-Arcia, A.V. (2019). Columnar cactus recognition in aerial images using a deep learning approach. *Ecological Informatics*, 52(2019), 131-138. DOI: <https://doi.org/10.1016/j.ecoinf.2019.05.005>.

McFeeters, S.K. (1996). The use of the Normalized Difference Water Index (NDWI) in the delineation of open water features. *International Journal of Remote Sensing*, 17(7), 1425-1432. DOI: <https://doi.org/10.1080/01431169608948714>.

Noi, P.T. & Kappas, M. (2017). Comparison of Random Forest, k-Nearest Neighbor, and Support Vector Machine Classifiers for land cover classification using Sentinel-2 Imagery. *Sensors*, 18(1), 18, 1-20. DOI: <https://doi.org/10.3390/s18010018>.

Pal, M., Akhsay, Rohilla, H. & Teja, B.C. (2020). Patch based land cover classification: A comparison of Deep Learning, SVM and NN classifiers. *IGARSS 2020-2020 IEEE International Geoscience and Remote Sensing Symposium*, 1933-1936. Waikoloa, Hawaii. USA. DOI: <https://doi.org/10.1109/IGARSS39084.2020.9323755>.

Qin, R. (2014). A mean shift vector-based shape feature for classification of high spatial resolution remotely sensed imagery. *IEEE Journal of Selected Topics in Applied Earth Observations and Remote Sensing*, 8(5), 1974-1985. DOI: <https://doi.org/10.1109/JSTARS.2014.2357832>.

Ramanath, A., Muthusrinivasan, S., Xie, Y., Shekhar, S. & Ramachandra, B. (2019). NDVI versus CNN features in Deep Learning for land cover classification of aerial images. *IGARSS 2019-2019 IEEE International Geoscience and Remote Sensing Symposium*, 6483-6486. Yokohama, Japan. DOI: <https://doi.org/10.1109/IGARSS.2019.8900165>.

Ratajczak, R., Crispim-Junior, C.F., Faure, E., Fervers, B. & Tougne, L. (2019). Automatic land cover

- reconstruction from historical aerial images: An evaluation of features extraction and classification algorithms. *IEEE Transactions on Image Processing*, 28(7), 3357-3371. DOI: <https://doi.org/10.1109/TIP.2019.2896492>.
- Thasveen, M.S. & Suresh, S. (2021). Land-use and land-cover classification methods: A review. *2021 Fourth International Conference on Microelectronics, Signals & Systems (ICMSS)*, 1-6. Kollam, India. DOI: <https://doi.org/10.1109/ICMSS53060.2021.9673623>.
- Xu, Z., Chen, J., Xia, J., Du, P., Zheng, H. & Gan, L. (2018). Multisource earth observation data for land-cover classification using random forest. *IEEE Geoscience and Remote Sensing Letters*, 15(5), 789-793. DOI: <https://doi.org/10.1109/LGRS.2018.2806223>.